NRIAG Journal of Astronomy and Geophysics (2016) 5, 48–54

National Research Institute of Astronomy and Geophysics

NRIAG Journal of Astronomy and Geophysics

www.elsevier.com/locate/nrjag

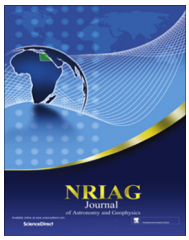

Derivation of the physical parameters for strong and weak flares from the H_α line

M.A. Semeida *, **M.G. Rashed**

Department of Solar and Space Research, National Research Institute of Astronomy and Geophysics, Helwan, Egypt

Received 24 November 2014; revised 11 April 2016; accepted 30 April 2016
Available online 24 May 2016

KEYWORDS

Solar flares;
Physical parameters;
H-alpha;
Spectral lines

Abstract The two flares of 19 and 30 July 1999 were observed in the H_α line using the multichannel flare spectrograph (MFS) at the Astronomical Institute in Ondřejov, Czech Republic. We use a modified cloud method to fit the H_α line profiles which avoids using the background profile. We obtain the four parameters of the two flares: the source function, the optical thickness at line center, the line-of-sight velocity and the Doppler width. The observed asymmetry profiles have been reproduced by the theoretical ones based on our model. A discussion is made about the results of strong and weak flares using the present method.

1. Introduction

Analysis of the H_α line profiles is a useful way for the determination of physical parameters in solar chromospheric structures. The method most frequently used, is known as the classical cloud model, which allows a simultaneous determination of four parameters: the source function, the optical thickness at line center, the line-of-sight velocity and the Doppler width. This method succeeds in inverting line profiles in chromospheric structures (Alissandrakis et al., 1990; Tsiropoula et al., 1993; Tsiropoula and Schmieder, 1997; Liu and Ding, 2001; Semeida, 2004; Semeida et al., 2005; Rashed, 2008). However, it is only effective for dark features on the disk, such as dark mottles of a chromospheric rosette region (e.g., Tsiropoula et al., 1993, 1999; Tsiropoula and Schmieder, 1997), superpenumbral fibrils and arch filament systems (e.g., Alissandrakis et al., 1990; Mein et al., 1996). The heights of these structures above the chromospheric base play a decisive role in shaping the observed profiles. The method of differential cloud models was proposed by Mein and Mein (1988), which takes into account the fluctuations of the chromospheric background in active regions and velocity shears inside the cloud, but it can only be applied to dark clouds in order to avoid singularities and eliminate spurious solutions. The method of multi-cloud model has been used to analyze the spectra of limb features, such as post-flare loops (e.g., Gu et al., 1997); however, this method may lead to meaningless solutions for the flare ribbons on the disk. In cases of bright features, the radiative and collisional damping effect may play an important role in the formation of the H_α line. Hence, the Voigt profile is more realistic than a Gaussian profile in the cloud model. Tsiropoula et al. (1999) approximated the Voigt

* Corresponding author.
Peer review under responsibility of National Research Institute of Astronomy and Geophysics.

http://dx.doi.org/10.1016/j.nrjag.2016.04.005

profile by the sum of a Doppler core and Lorentzian damping wings and considered the variation of the source function with optical thickness. In this method, the theoretical profiles have a singularity in Lorentzian damping wings (where the denominator equals zero) which causes a poor fit if assuming a constant source function. Some authors have investigated the variations of the source function with the opacity of the structures (Mein et al., 1996; Paletou, 1997), and the cloud model is extended to cases of non-constant source functions (Zhang et al., 1987; Mein et al., 1996; Tsiropoula et al., 1999). However, the adoption of a non-constant source function yields only little improvement in the case of a low opacity. Note also that the H_α source function is sensitive to larger macroscopic velocities of the order of a few tens of km s^{-1}, but this effect is less important for high electron densities where the collisional excitation plays a significant role (Heinzel et al., 1999). Here we still use a constant source function to analyze the line spectra. In this sense, the value of the source function that we obtain reflects a mean value averaged over a specific region.

Concerning solar flares, the most obvious signature of H_α line profiles is the red asymmetry, which has been interpreted as a consequence of downflows related to the chromospheric condensation (e.g., Ichimoto and Kurokawa, 1984; Canfield et al., 1987; Gan and Fang, 1990; Ding et al., 1995; Cauzzi et al., 1996). In this work we pay special attention to the origin of the line asymmetry and use a new method to analyze the H_α profiles in strong and weak flaring regions. This method avoids using a background profile which is usually hard to determine. Two-dimensional parameters are deduced, based on the 2D spectra of the flaring regions and the results are useful for a better understanding of the flare dynamics.

2. Observations and data reduction

The newly rebuilt multichannel flare spectrograph (MFS) at Ondřejov Observatory (Kotrč et al., 1992) was used to take a time series of H_α line spectra of a flare in the active region NOAA 8636 located at N21 E58 on 19 July 1999. The observing time is from 08:16:30 UT to 10:56:00 UT and according to the Solar Geophysical Data, the flare began at 08:19:00 UT and ended at 10:58:00 UT, reaching its maximum at 08:35:00 UT, and it was an event with H_α importance 2N and soft X-ray class M5.8. Also, the H_α flare spectra of 30 July, 1999 taken during the time interval from 08 h:51 m:00 s UT to 08 h:52 m:30 s UT in the active region NOAA 8651 located at N24 E44. According to the Solar Geophysical Data this flare starts at 08 h:47 m:00 s UT, ended at 09 h:06 m:00 s UT, reaching its maximum at 08 h:52 m:00 s UT and it was an event with H_α importance SN and soft X-ray class C5.4. The output from the ordinary video cameras is a TV image with a rectangular frame, the ratio of the sizes being 4.0:3.0. The system of observation works with the frequency of 25 pictures/s, and each picture has horizontal lines. Chips of CCD cameras are usually ½″ in diagonal (6.4 × 4.8 mm) or 1/3″ (4.8 × 3.6 mm) with various numbers of the chip pixels. After we digitized and processed spectra we corrected it by getting the dispersion curve and calibrated it by getting a very good calibration curve for all of H_α line spectra of our studied flare. Then we reduced it by subtracting the undisturbed profile near the flaring region to get the H_α line profile spectra.

3. Method of spectral analysis

The classical cloud model adopts a mean profile over the quiet chromosphere as the background profile. However, for flares it is not feasible because of the large fluctuations in the active-region background. Here we use a technique avoiding the use of a background profile (Liu and Ding, 2001; Semeida, 2004, 2008; Semeida et al., 2005).

In the Cloud model, the line intensity is given by

$$I(\Delta\lambda) = I_o(\Delta\lambda)e^{-\tau(\Delta\lambda)} + S_o[1 - e^{-\tau(\Delta\lambda)}], \quad (1)$$

where the source function S_o is assumed to be constant and frequency independent, $I_o(\Delta\lambda)$ is the background intensity and $\tau(\Delta\lambda)$ is the optical thickness which is expressed as follows:

$$\tau(\Delta\lambda) = \tau_o H(a, x) \quad (2)$$

where $H(a, x)$ is the Voigt profile and given by

$$H(a, x) = a/\pi \int_{-\infty}^{+\infty} \frac{e^{-y^2}}{a^2 + (x - y)^2} dy \quad (3)$$

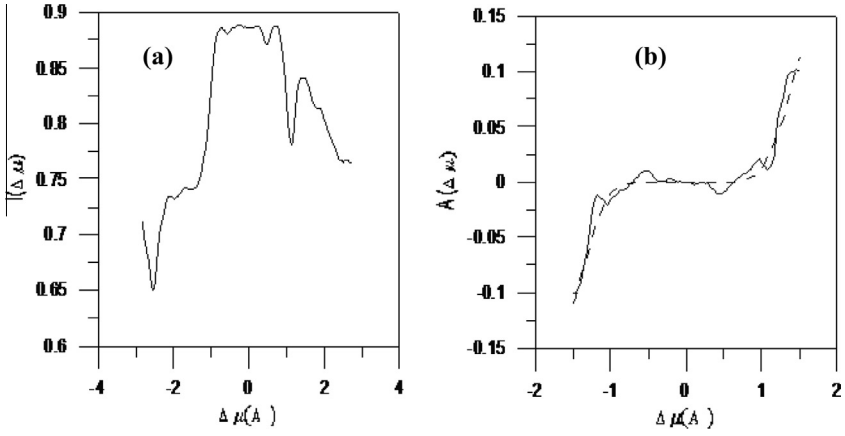

Figure 1 Strong flare (July 19, 1999). (a) Atypical H_α line profile with asymmetry in the flaring region at time 08:36:35 UT. (b) Comparison between the asymmetry profile observed (solid line) and the fitted one (dotted line). The intensity is normalized to the continuum near the H_α line.

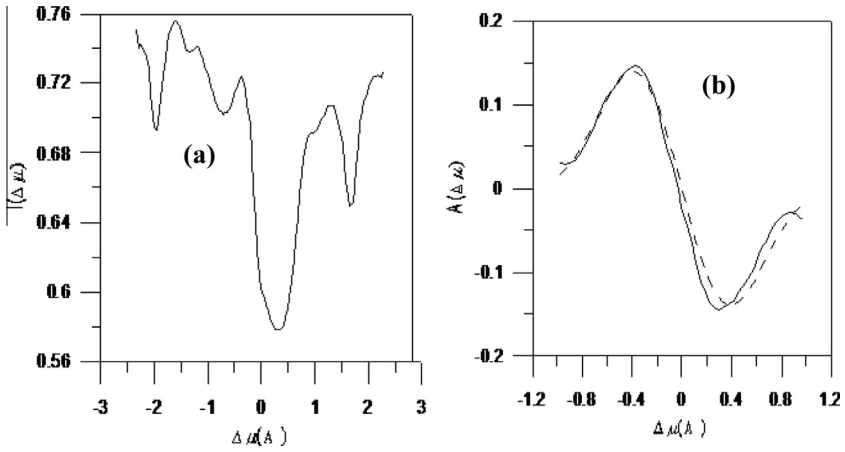

Figure 2 Strong flare (July 19, 1999). (a) Atypical H_α line profile with asymmetry in flaring region at time 08:47:50 UT. (b) Comparison between the asymmetry profile observed (solid line) and the fitted one (dotted line). The intensity is normalized to the continuum near the H_α line.

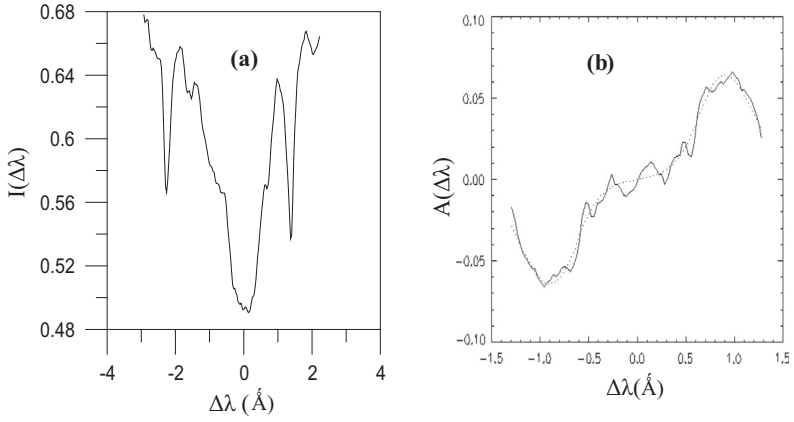

Figure 3 Weak flare (July 30, 1999). (a) Atypical H_α line profile with asymmetry in the flaring region at time 08:51:51 UT. (b) Comparison between the asymmetry profile observed (solid line) and the fitted one (dotted line). The intensity is normalized to the continuum near the H_α line.

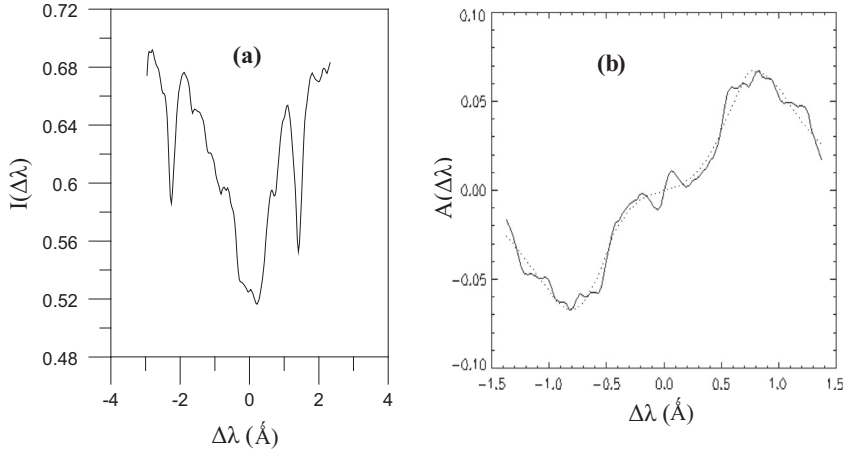

Figure 4 Weak flare (July 30, 1999). (a) Atypical H_α line profile with asymmetry in the flaring region at time 08:51:52 UT. (b) Comparison between the asymmetry profile observed (solid line) and the fitted one (dotted line). The intensity is normalized to the continuum near the H_α line.

Table 1 Physical parameters derived from the modified Cloud model method for the flare on 19 July 1999.

Time observation h:m:s	Source function	Optical thickness	Line shift	Doppler width	Velocity (K/s)
8:36:35	1.1	0.44	1.71	0.46	78
8:36:45	0.7	1.05	0.92	0.51	42
8:36:50	0.6	0.51	0.84	0.46	38
8:37:00	0.56	0.22	0.76	0.58	35
8:40:05	0.92	1.33	0.8	0.39	37
8:40:20	0.7	0.3	0.91	0.38	42
8:40:40	0.9	1.05	0.86	0.29	39
8:41:00	0.93	0.38	0.98	0.4	45
8:42:20	0.87	0.95	0.98	0.4	45
8:43:50	0.87	1.21	0.85	0.38	39
8:45:35	0.45	0.45	0.86	0.53	39
8:46:10	1.06	0.62	0.79	0.46	36
8:46:15	0.87	1.31	0.8	0.46	37
8:46:20	3.4	0.06	0.82	0.23	38
8:46:50	1.22	0.33	0.8	0.44	36
8:47:20	1.14	0.46	0.79	0.44	36
8:47:25	1.05	0.55	0.82	0.48	37
8:47:30	1.03	0.79	0.73	0.56	33

where

$$x = \frac{\Delta\lambda - \Delta\lambda_I}{\Delta\lambda_D} \tag{4}$$

$$a = \frac{\Gamma\lambda_o^2}{4\pi c\Delta\lambda_D} \tag{5}$$

In the above equations, Γ is the damping constant (this parameter has no essential impact on the other parameters to be fitted, thus in the computations Γ is fixed to be a value of $5 \times 10^9\ s^{-1}$, considering both the radiative damping and the collisional broadening).

The four unknown parameters are the source function, S_o, the optical thickness at line center, τ_o, the Doppler shift, $\Delta\lambda_I$ and the Doppler width, $\Delta\lambda_D$, which are assumed to be constant throughout the perturbed layer.

Below the perturbed layer, the H_α line profile is assumed to be symmetric, namely,

$$I_o(\Delta\lambda) = I_o(-\Delta\lambda) \tag{6}$$

$$I(-\Delta\lambda) = I_o(\Delta\lambda)e^{-\tau(-\Delta\lambda)} + S_o[1 - e^{-\tau(-\Delta\lambda)}] \tag{7}$$

Subtraction of $I(-\Delta\lambda)$ from $I(\Delta\lambda)$ leads to an asymmetry profile,

$$\Delta I(\Delta\lambda) = [I_o(\Delta\lambda) - S_o][e^{-\tau(\Delta\lambda)} - e^{-\tau(-\Delta\lambda)}] \tag{8}$$

From Eqs. (1) and (8) we can eliminate the background profile $I_o(\Delta\lambda)$, then we get:

$$A(\Delta\lambda) \equiv \Delta I(\Delta\lambda) = [I(\Delta\lambda) - S_o][1 - e^{\tau(\Delta\lambda)-\tau(-\Delta\lambda)}] \tag{9}$$

Using the above formula, we have tried to fit the observed asymmetry profile by utilizing an iterative least square procedure of the Levenberg–Marquardt method for nonlinear functions. To check the validity of this method, we have constructed theoretical asymmetry profiles by choosing different sets of the four parameters, which can in most cases be recovered using this method.

Table 2 Physical parameters derived from the modified Cloud model method for the flare on July 30, 1999.

Time h:m:s	Source function (S_0)	Optical thickness τ_0	Line shift $\Delta\lambda_I$	Doppler width $\Delta\lambda_D$	Velocity (km/s)
08:51:00	0.54137845	0.15308238	0.63667933	0.58302019	29.103
08:51:10	0.055452912	0.61735206	0.76528543	0.36632057	34.983
08:51:18	36.764134	0.0013586818	0.83068286	0.44810613	37.9722
08:51:19	0.25191168	0.27098508	0.51065285	1.0726531	23.343
08:51:21	0.34351381	3.8555628	0.035746789	0.75169916	1.634
08:51:22	0.58463346	0.13615305	0.71145091	0.50311608	32.521
08:51:28	0.42167650	0.12589537	0.89461055	0.37698223	40.895
08:51:29	0.59950396	0.14033322	0.93874145	0.60235696	42.912
08:51:30	0.68784361	0.072404627	0.59416683	0.43917158	27.1606
08:51:33	0.31468614	0.15523410	0.70129134	0.42554497	32.058
08:51:34	0.54967255	0.025001983	0.86380003	0.16883807	39.486
08:51:37	0.55528314	0.090780213	0.76909675	0.53286872	35.157
08:51:40	0.18185715	1.2489180	0.34365351	2.1469488	15.709
08:51:41	0.41330298	2.0269759	0.069676228	0.93383751	3.185
08:51:42	0.78035765	0.075203219	0.88437647	0.40758575	40.427
08:51:43	0.48905376	0.16007342	0.83136164	0.43140672	38.003
08:51:44	0.36916438	0.59075209	0.29366295	0.42189543	13.424
08:51:46	0.34220213	0.23404004	0.88870497	0.40859731	40.625
08:51:47	0.48297014	0.23902349	0.60024817	0.41273561	27.439
08:51:49	0.44551057	0.14926339	0.80836100	0.36590109	36.952
08:51:51	0.52569513	0.14282723	0.86646722	0.45789213	39.608
08:51:52	0.40737531	1.9931776	0.058747479	0.86049327	2.685
08:51:53	0.65876352	0.089186764	0.95989737	0.57298462	43.879
08:51:56	0.43510169	0.22492042	0.62459439	0.36175719	28.552
08:51:57	0.64294705	0.10096193	0.87576192	0.62632470	40.033
08:51:58	0.50853424	1.3636842	0.062820744	0.86425757	2.872
08:51:59	0.41057247	0.17481827	0.89395745	0.31621744	40.865
08:52:00	0.34704751	0.17881455	0.85334008	0.45394260	39.008

The initial values of the parameters for the iteration are taken in the following way.

- The intensity near the H_α continuum for the source function.
- One for the optical thickness at line center.
- 1 Å for the Doppler shift.
- 0.4 Å for the Doppler width.

It should be emphasized that the computation converges rapidly and varying the initial values has almost no influence on the finally converged data.

4. Results and discussion

We apply the method described above to the observed H_α line profiles which show red asymmetries, while the line center is nearly not shifted. Figs. 1 and 2 show a typical line profile with red asymmetry for strong flare, and also Figs. 3 and 4 explain a typical line profile with red asymmetry for weak flare, along with the asymmetry profile defined by Eq. (9). The asymmetry profiles from our observations can be well fitted based on the modified cloud method, where we eliminate the influence of other spectral lines. The asymmetry diminishes with time, so the method should be used with caution where the asymmetry profile cloud model becomes very flat. In this case $A(\Delta\lambda)$ approaches to 0, which will induce poor convergence and meaningless solutions.

In our work, we selected some frames of 2D spectral data of strong flare for study, which are corresponding to the profiles from time at 8 h:36 m:35 s to time at 8 h:46 m:10 s. The physical parameters, the source function, the optical thickness, the Doppler shift, and the Doppler width for the H_α line profiles derived from the modified Cloud model method are shown in Table 1 and also, we selected some profiles of our observed spectral data for study from time at 8 h:51 m:00 s to time at 8 h:52 m:00 s for weak flare. Table 2 gave the physical parameters: the source function, the optical thickness, the Doppler shift, Doppler width and the downward velocity for the H_α line profiles of it.

The average temporal variation of the source function, the optical thickness, the Doppler shift and the Doppler width of the H_α line profiles of a strong flare on 19 July 1999, which we got by using the modified cloud method give the following results:

* The flare arrived its maximum after the time 08:40:05 UT.
* The variations of the four parameters are roughly similar during the time of observations, which imply that the two kernels may be heated by the same mechanism.

But for the weak flare of 30 July 1999, we found that:

* The flare is arrived to its maximum after the time 08:52:00 UT.
* The downward motion abruptly increases at the onset of the flare, and then it increases gradually and remains fairly large in the later phase, which is in agreement with the result of Ichimoto and Kurokawa (1984) and Liu and Ding (2001).

From the intrinsic factor, the absorption coefficient is given by the following relation:

$$a(\Delta\lambda) = \frac{\pi^{1/2} e^2 \lambda^2 f H(a,x)}{m_e c^2 \Delta\lambda_D} n_2, \tag{10}$$

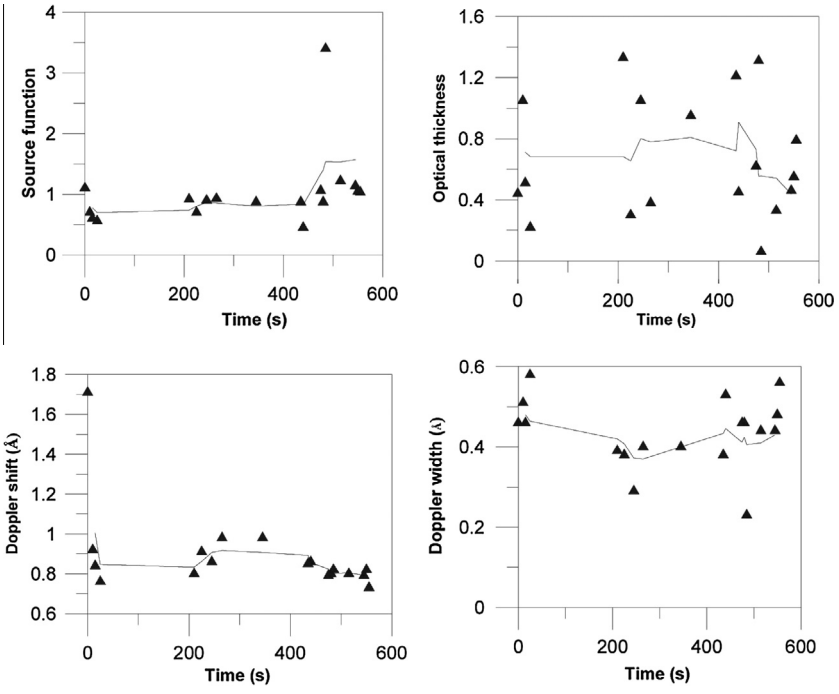

Figure 5 The average temporal variation of the physical parameters of the H_α line profiles of the flare of July 19, 1999.

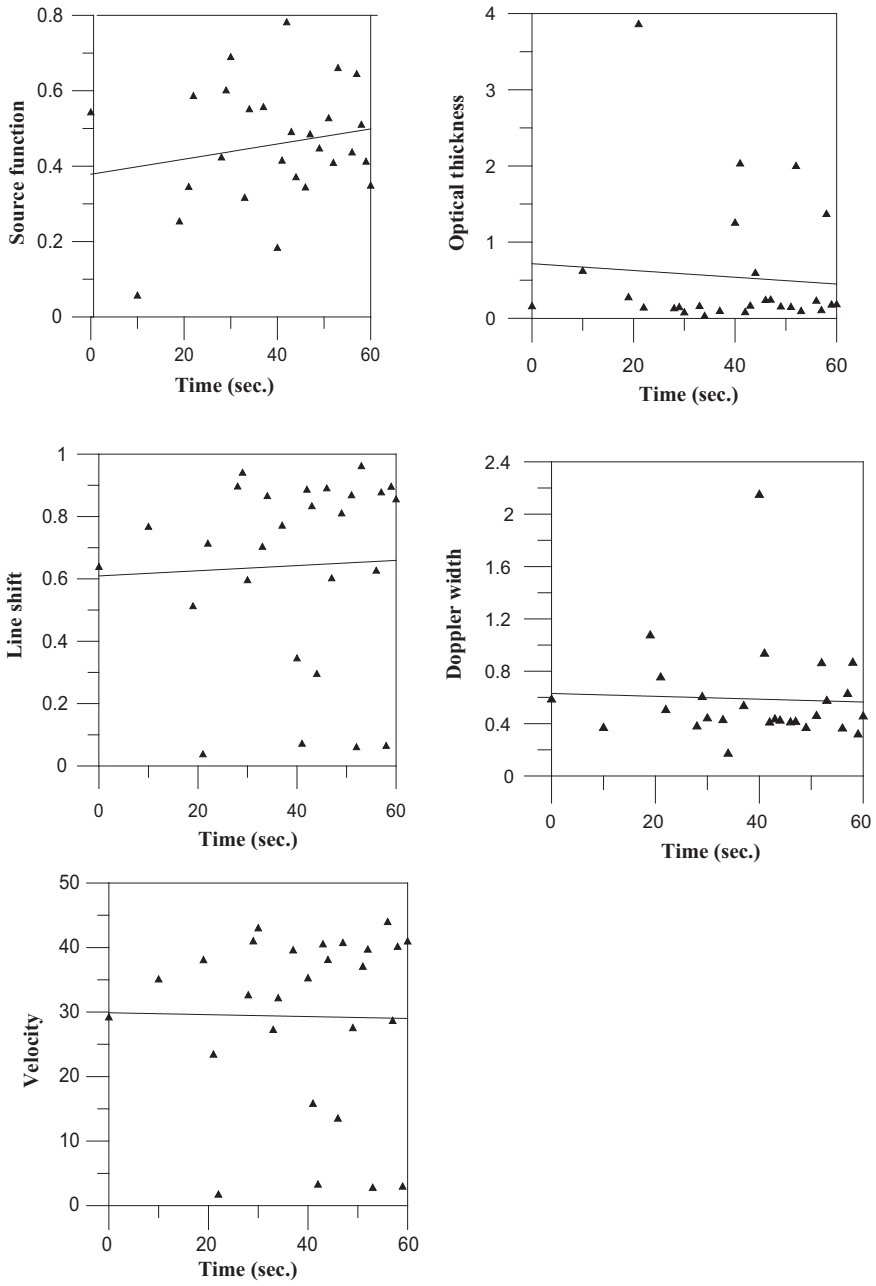

Figure 6 The average temporal variation of the physical parameters of the H_α line profiles of the weak flare of July 30, 1999.

where $f = 0.641$ is the oscillator strength for the H_α. And the optical thickness at the line center is given by the following relation:

$$\tau_0 = a(0)d \sim \frac{n_2 d}{\Delta\lambda_D}, \tag{11}$$

where n_2 is the number density in the second level of hydrogen and d is the geometrical thickness of the structure along the line of sight. If the value of $n_2 d$ does not vary appreciably, there should exist an anticorrelation between τ_o and $\Delta\lambda_D$. However, in the case of solar flares, the value of n_2 is greatly enhanced because of the non-thermal excitation of the hydrogen atoms caused by precipitating high-energy electrons. The value of d could also suffer a pronounced change, because the condensation is confined in a narrow layer when it is initially formed (Fisher et al., 1985), but dissipates gradually during its downward propagation. Therefore, it is conceivable that the optical thickness is proportional to the Doppler width in the case of solar flares.

It seemed that the asymmetry of the observed profiles is of a great significance of the used modified cloud method, and therefore the red asymmetry has been interpreted by various authors as a consequence of the chromospheric condensation, which originates primarily at the top of the chromosphere and propagates downward (Ichimoto and Kurokawa, 1984; Canfield et al., 1987; Gan and Fang, 1990; Ding et al., 1995; Cauzzi et al., 1996).

The asymmetry only occurs at the line wings and there is nearly no shift at the line center, which has been frequently argued (Fang et al., 1992; Ding et al., 1995).

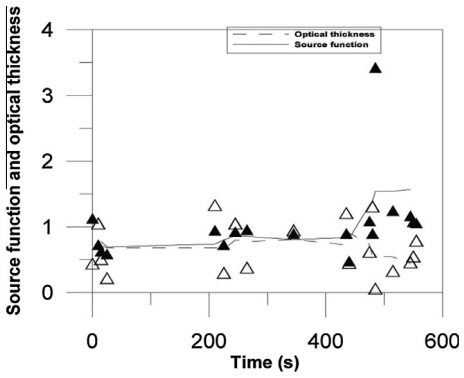

Figure 7 The average temporal variation of the source function and the optical thickness (in unit of $I_{\text{continuum}}$) of the H_α line profiles of the flare of July 19, 1999.

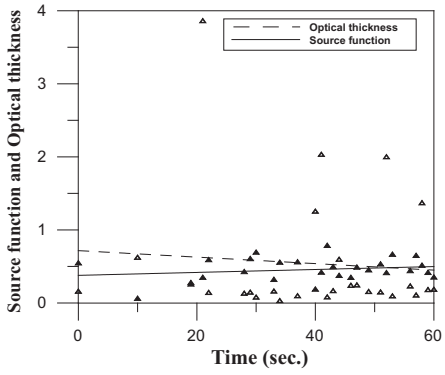

Figure 8 The average temporal variation of the source function and the optical thickness (in unit of $I_{\text{continuum}}$) of the H_α line profiles of the flare of July 30, 1999.

* The source function and the Doppler width roughly depend on each other but some authors have pointed out that they should depend on each other (Durrant, 1975; Cram, 1986).
* A good agreement proportional relation between the source function and the optical thickness at the line center, comparing with the result mentioned by Heinzel et al. (1999), Liu and Ding (2001) for the strong flare is shown in Fig. 8.
* But for the weak flare the variations of the four parameters are roughly similar during the time of observations as shown in Fig. 7, which implies that the two kernels may be heated by a same mechanism, also the average temporal variation of the source function and the optical thickness at the line center, illustrated proportional relation between them as shown in Fig. 8 roughly in comparison with the strong flare (see Figs. 5 and 6).

5. Conclusion

We have used a new method to derive the physical parameters, the source function, the optical thickness at line center, the Doppler shift and the Doppler width of the chromospheric strong and weak flares spectral data observed on 19 and 30 July 1999 respectively with the multichannel flare spectrograph (MFS) at the Astronomical Institute in Ondřejov, Czech Republic.

The average temporal variation of the source function and the optical thickness at the line center, illustrates a good proportional relation between them as shown in Fig. 7 more than for the weak flare as illustrated in Fig. 8, comparing with the roughly proportional relation of Heinzel et al. (1999) and Liu and Ding (2001). Although this method is known to be applicable used for weak flares, it gave interesting results for our studied strong flare. This method can also be applied to other chromospheric structures as long as the profiles are asymmetric. The source function we finally obtain is greater than $I_o(\Delta\lambda)$ near the line core, which implies a property of excess emission in the red wing.

References

Alissandrakis, C.E., Tsiropoula, G., Mein, P., 1990. Astron. Astrophys. 230, 200.
Canfield, R.C., Metcalf, T.R., Strong, K.T., Zarro, D.M., 1987. Nature 326, 165.
Cauzzi, G., Falchi, A., Falciani, R., Smaldone, L.A., 1996. Astron. Astrophys. 306, 625.
Cram, L.E., 1986. Astrophys. J. 300, 830.
Ding, M.D., Fang, C., Huang, Y.R., 1995. Sol. Phys. 158, 81.
Durrant, C.J., 1975. Sol. Phys. 44, 41.
Fang, C., Falciani, R., Smaldone, L.A., 1992. Astron. Astrophys. 256, 255.
Fisher, G.H., Canfield, R.C., McClymont, A.N., 1985. Astrophys. J. 289, 414.
Gan, W.Q., Fang, C., 1990. Chin. J. Astron. Astrophys. 14, 413.
Gu, X.M., Ding, Y.J., Luo, Z., Schmieder, B., 1997. Astron. Astrophys. 324, 289.
Heinzel, P., Mein, N., Mein, P., 1999. Astron. Astrophys. 346, 322.
Ichimoto, K., Kurokawa, H., 1984. Sol. Phys. 93, 105.
Kotrč, P., Heinzel, P., Knizek, M., 1992. Joso Annual Report 1992, p. 114.
Liu, Y., Ding, M.D., 2001. Sol. Phys. 200, 127.
Mein, P., Mein, N., 1988. Astron. Astrophys. 203, 162.
Mein, N., Mein, P., Heinzel, P., Vial, J.-C., Malherbe, J.M., Staiger, J., 1996. Astron. Astrophys. 309, 275–283.
Paletou, F., 1997. Astron. Astrophys. 317, 244.
Rashed, M.G., Ph.D., 2008. Dept. of Astronomy, Faculty of Science, Al-Azhar University.
Semeida, M.A., Ph.D., 2004. Dept. of Astronomy, Faculty of Science, Cairo University and Ondrjov Observatory.
Semeida, M.A., Galal, A.A., Rassem, M.A., Sabry, M., 2005. ESA SP-596.
Tsiropoula, G., Alissandrakis, C.E., Schmieder, B., 1993. Astron. Astrophys. 271, 574.
Tsiropoula, G., Madi, C., Schmieder, B., 1999. Sol. Phys. 187, 11.
Tsiropoula, G., Schmieder, B., 1997. Astron. Astrophys. 324, 1183.
Zhang, Q.Z., Livingston, W.C., Hu, J., Fang, C., 1987. Sol. Phys. 114, 245.